EXHIBIT C

Low-density lipoprotein receptor-related protein 5 (LRP5) is essential for normal cholesterol metabolism and glucose-induced insulin secretion

Takahiro Fujino[a,b], Hiroshi Asaba[b,c], Man-Jong Kang[b,d], Yukio Ikeda[a,b,c], Hideyuki Sone[a,b], Shinji Takada[e,f,g], Dong-Ho Kim[a], Ryoichi X. Ioka[a], Masao Ono[h], Hiroko Tomoyori[i], Minoru Okubo[j], Toshio Murase[j], Akihisa Kamataki[a], Joji Yamamoto[a,c], Kenta Magoori[a], Sadao Takahashi[k], Yoshiharu Miyamoto[h], Hisashi Oishi[h], Masato Nose[h], Mitsuyo Okazaki[l], Shinichi Usui[l], Katsumi Imaizumi[i], Masashi Yanagisawa[c,m], Juro Sakai[a,c,n], and Tokuo T. Yamamoto[a]

[a]Gene Research Center and Division of Nephrology, Endocrinology, and Vascular Medicine, Department of Medicine, Tohoku University, Sendai 980-8574, Japan; [c]Yanagisawa Orphan Receptor Project, Exploratory Research for Advanced Technology, Japan Science and Technology Corporation, Tokyo 135-0064, Japan; [d]Department of Animal Science, College of Agriculture, Chonnam National University, Kwangju 500-600, Korea; [e]Graduate School of Science, Kyoto University, Kyoto 606-8502, Japan; [f]Kondoh Differentiation Signaling Project, Exploratory Research for Advanced Technology, Japan Science and Technology Corporation, Kyoto 606-8305, Japan; [g]Center for Integrative Bioscience, Okazaki, Aichi 444-8585, Japan; [h]Departments of Pathology and Orthopedics, Ehime University School of Medicine, Ehime 791-0295, Japan; [i]Laboratory of Nutritional Chemistry, Graduate School of Agriculture, Kyusyu University, Fukuoka 812-8581, Japan; [j]Department of Endocrinology and Metabolism, Toranomon Hospital, Tokyo 105-8470, Japan; [k]Third Department of Internal Medicine, Fukui Medical University, Fukui 910-1193, Japan; [l]Laboratory of Chemistry, College of Liberal Arts and Sciences, Tokyo Medical and Dental University, Chiba 282-0827, Japan; and [m]Howard Hughes Medical Institute, Department of Molecular Genetics, University of Texas Southwestern Medical Center, Dallas, TX 75235-9050

Edited by Michael S. Brown, University of Texas Southwestern Medical Center, Dallas, TX, and approved November 7, 2002 (received for review June 26, 2002)

A Wnt coreceptor low-density lipoprotein receptor-related protein 5 (LRP5) plays an essential role in bone accrual and eye development. Here, we show that LRP5 is also required for normal cholesterol and glucose metabolism. The production of mice lacking LRP5 revealed that LRP5 deficiency led to increased plasma cholesterol levels in mice fed a high-fat diet, because of the decreased hepatic clearance of chylomicron remnants. In addition, when fed a normal diet, LRP5-deficient mice showed a markedly impaired glucose tolerance. The LRP5-deficient islets had a marked reduction in the levels of intracellular ATP and Ca^{2+} in response to glucose, and thereby glucose-induced insulin secretion was decreased. The intracellular inositol 1,4,5-trisphosphate (IP3) production in response to glucose was also reduced in LRP5−/− islets. Real-time PCR analysis revealed a marked reduction of various transcripts for genes involved in glucose sensing in LRP5−/− islets. Furthermore, exposure of LRP5+/+ islets to Wnt-3a and Wnt-5a stimulates glucose-induced insulin secretion and this stimulation was blocked by the addition of a soluble form of Wnt receptor, secreted Frizzled-related protein-1. In contrast, LRP5-deficient islets lacked the Wnt-3a-stimulated insulin secretion. These data suggest that Wnt/LRP5 signaling contributes to the glucose-induced insulin secretion in the islets.

diabetes | Wnt protein | chylomicron remnant | pancreatic β cells | insulin-like growth factor 1

Low-density lipoprotein (LDL) receptor-related protein (LRP)5 and LRP6 are coreceptors involved in the Wnt signaling pathway (1–6). The Wnt signaling pathway plays a pivotal role in embryonic development (7, 8) and oncogenesis (9) through various signaling molecules including Frizzled receptors (10), recently characterized LRP5 and LRP6 (1–6), and Dickkopf proteins (4, 6). In addition, the Wnt signaling is also involved in adipogenesis by negatively regulating adipogenic transcription factors (Tcfs) (11). Although Wnt signaling has been characterized in both developmental and oncogenic processes, little is known about its function in the normal adult.

Recent studies have revealed that loss of function mutations in the LRP5 gene cause the autosomal recessive disorder osteoporosis–pseudoglioma syndrome (12). LRP5 is expressed in osteoblasts and transduces Wnt signaling via the canonical pathway, thereby modulating bone accrual development (12, 13). A point mutation in a "propeller" motif in LRP5 causes a dominant-positive high bone density by impairing the action of a normal antagonist of the Wnt pathway, Dickkopf, thereby increasing Wnt signaling (14, 15). In addition, the human LRP5 gene is mapped within the region (IDDM4) linked to type 1 diabetes on chromosome 11q13 (16).

In previous studies, we and others showed that LRP5 is highly expressed in many tissues, including hepatocytes and pancreatic beta cells (17, 18). We also showed that LRP5 can bind apolipoprotein E (apoE) (18). This finding raises the possibility that LRP5 plays a role in the hepatic clearance of apoE-containing chylomicron remnants, a major plasma lipoprotein carrying diet-derived cholesterol.

To evaluate the *in vivo* roles of LRP5, we generated LRP5-deficient mice. In this paper, we describe a function of LRP5 in the metabolism of cholesterol and glucose. Our data indicate that LRP5 is a multifunctional receptor involved in multiple pathways, including bone development, cholesterol metabolism, and the modulation of glucose-induced insulin secretion.

Experimental Procedures

Generation of LRP5-Deficient Mice. To produce mice carrying a mutated LRP5 gene, a targeting vector was constructed from a genomic DNA fragment containing exons 17 and 18 of the murine LRP5 gene. A neomycin-resistance gene under transcriptional control of the mouse phosphoglycerate kinase-1 promoter (PGK-neo) was inserted into the *Xho*I site within exon 18 of the mouse LRP5 gene. The 5′ and 3′ DNA fragments flanking PGK-neo were ligated into a pMCDT-A plasmid (GIBCO/BRL) composed of a poly(A)-less *neo* gene, a polymerase destabilizing signal, a pausing signal for RNA polymerase II, and the diphtheria toxin A fragment (DT-A) gene for negative selection (19). TT2 embryonic stem (ES) cells (20) were

This paper was submitted directly (Track II) to the PNAS office.

Abbreviations: apoE, apolipoprotein E; $[Ca^{2+}]_i$, intracellular Ca^{2+} concentration; CM, conditioned medium; HNF, hepatocyte nuclear factor; IGF, insulin-like growth factor; IRS, insulin receptor substrate; IP3, inositol 1,4,5-trisphosphate; LDL, low-density lipoprotein; LRP, LDL receptor-related protein; sFRP-1, secreted Frizzled-related protein-1; Tcf, transcription factor.

[b]T.F., H.A., M.-J.K., Y.I., and H.S. contributed equally to this work.

[n]To whom correspondence should be addressed at: Yanagisawa Orphan Receptor Project, Exploratory Research for Advanced Technology (ERATO), Japan Science and Technology Corporation (JST), National Museum of Emerging Science and Innovation, 2-41, Aomi, Koto-ku, Tokyo 135-0064, Japan. E-mail: jmsakai@mail.cc.tohoku.ac.jp or jmsakai@orphan.miraikan.jst.go.jp.

transfected using standard techniques (21). Chimeric males were generated using the morula aggregation technique, and mated to C57BL/6J female mice. After achieving germ-line transmission, LRP5+/− females were crossed with C57BL/6J males. For immunoblotting, an antibody against murine LRP5 peptide (ATLYPPILNPPPSPA, amino acids 1490–1504, NCBI Protein database accession no. NP_032539) was generated. The antibody binding was detected with a chemiluminescence detection kit (ECL, no. RPN2106, Amersham Pharmacia Biotech).

Plasma Clearance and Hepatic Uptake of Chylomicron Remnants. Chylomicron remnants were prepared using a modified method of Redgrave and Martin (22) using functionally hepatectomized rats, and labeled with fluorescent lipid (1,1′-dioctadecyl-3,3,3′,3′-tetramethylindocarbocyanine perchlorate, DiI) as described by Takahashi *et al.* (23). Mice fed a high-fat diet for 16 weeks were injected i.v. into a femoral vein, with fluorescent chylomicron remnants from rat (5 μg per mouse) in 0.2 ml of PBS. Blood was sampled at various times and, after extracting lipid, plasma fluorescence was measured with a spectrofluorometer. The amount of fluorescence remaining in the plasma is expressed as a percentage of the calculated initial blood concentration, assuming that plasma volume is 4.4% (vol/wt) of body weight. After collection of the final blood samples, the mice were exsanguinated and livers were excised for the extraction of lipids and measurement of fluorescence.

Blood Glucose and Serum Insulin. Mice (6–8 months old) were fasted for 12 h and then given an i.p. injection of glucose (1 g/kg of body weight). Blood samples were obtained from the tail vein at the indicated times after the glucose load. Blood glucose and plasma insulin levels were measured with the Glucose CII test Wako (Wako Pure Chemical, Osaka) and an insulin RIA kit (Shionogi, Osaka), respectively.

Analysis of Pancreatic Islets. The procedure for the isolation of pancreatic islets is described in *Supporting Methods*, which is published as supporting information on the PNAS web site, www.pnas.org. For the measurement of insulin secretion from islets, pancreatic islets from 6- to 8-month-old mice were pooled and cultured in RPMI medium 1640 containing 11.6 mM glucose, 1% penicillin–streptomycin, 10% FBS, and 25 mM Hepes at pH 7.4 (medium A). Pancreatic islets cells were infected with recombinant adenoviruses encoding LRP5 (AdLRP5) (18) or LacZ (AdLacZ) according to the procedure by Becker *et al.* (24). After culturing for 16–20 h, islets were transferred to Krebs–Ringer buffer (KRB; Sigma) containing 0.2% BSA for the measurement of insulin secretion studies by using an RIA kit (Amersham Pharmacia Biotech). For measurement of intracellular Ca^{2+} concentration ($[Ca^{2+}]_i$), pancreatic islet cells were cultured on a collagen-coated, glass-bottomed well for 16 h in medium A, and loaded with the fluorescent Ca^{2+} indicator Fluo3/AM as described by Katoh *et al.* (25). Changes in $[Ca^{2+}]_i$ were measured using a confocal laser scanning microscope (Axiovert 100, Zeiss) with a ×40 objective lens. Intracellular levels of ATP and ADP were measured with a luciferase–luciferin system by using an ATP determination kit (catalog number A-22066, Molecular Probes; ref. 26). Intracellular levels of inositol 1,4,5-trisphosphate (IP3) were determined using an IP3 RIA kit (Amersham Pharmacia Biotech).

Wnt-Conditioned Media (CM) and Purified Secreted Frizzled-Related Protein-1 (sFRP-1). CM from Wnt-3a, Wnt-5a, and parental vector-transfected L cells were prepared according to Shibamoto *et al.* (27). CM were diluted 5-fold with medium A. After incubation with CM for 16 h, islets were transferred to Krebs–Ringer buffer for the measurement of insulin for secretion studies.

An expression plasmid encoding recombinant sFRP-1 containing Myc/polyhistidine epitopes (28) was used to produce recombinant sFRP-1 in COS7 cells. COS7 cells were transfected with the expression plasmid by using the Lipofectamine reagent (GIBCO/BRL). Twenty-four hours after the transfection, the cells were switched to a serum-free medium (OPTI-PRO, GIBCO/BRL) and cultured for 48 h. Recombinant sFRP-1 was purified from the culture medium of transfected cells by using a HisTrap kit (Amersham Pharmacia Biotech) according to the manufacturer's protocol. The purity of the purified protein was verified by immunoblot analysis with anti-Myc tag antibody (Cell Signaling Technology, Beverly, MA).

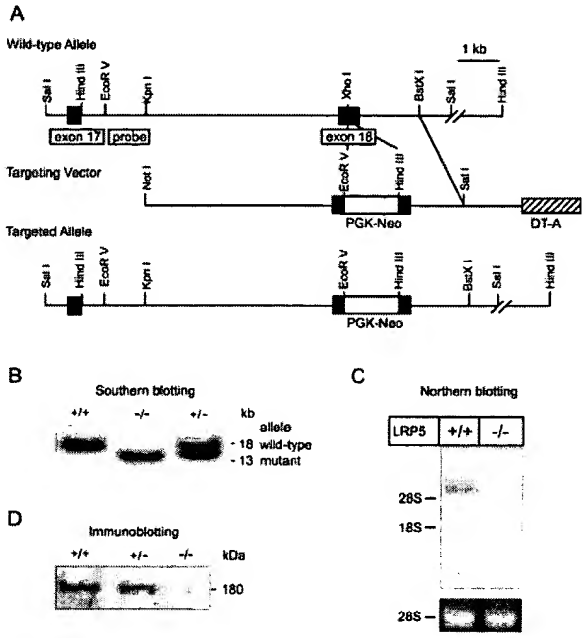

Fig. 1. Generation of LRP5-deficient mice. (*A*) Diagram of the targeting strategy. Only the relevant restriction sites are indicated. (*B*) Southern blot analysis of *Hin*dIII-digested DNA from LRP5+/+, LRP5−/−, and LRP5+/− mice. Southern blotting was performed with the probe indicated in *A*. *Hin*dIII digestion resulted in an 18-kb fragment in wild-type DNA and a 13-kb fragment in homologous recombinants. A typical autoradiogram is shown. (*C*) Northern blot analysis of LRP5 transcripts. Total RNA (15 μg) from the livers of LRP5+/+ and LRP5−/− mice was hybridized with a mouse LRP5 cDNA probe (extended from nucleotide 2401 to nucleotide 2991). A typical autoradiogram (48-h exposure) is shown. RNA loading was consistent among the lanes as judged by ethidium bromide staining and reprobing with glyceraldehyde-3-phosphate dehydrogenase. (*D*) Immunoblot analysis, using an anti-mouse LRP5 antibody, of LRP5+/+, LRP5+/−, and LRP5−/− mouse liver membrane fractions. Each lane was loaded with 500 μg of crude membrane fraction from the liver homogenates. Protein loading was consistent among the lanes as judged by Ponceau staining.

Results

Generation of LRP5-Deficient Mice. An insertion-type vector was constructed to disrupt an exon encoding a ligand-binding repeat of the mouse LRP5 gene (exon 18; Fig. 1*A*). Three lines of mice lacking LRP5 were identified by Southern blotting (Fig. 1*B*), and the absence of LRP5 transcripts (Fig. 1*C*) and protein (Fig. 1*D*) in the liver was confirmed by Northern blot and immunoblot analyses, respectively.

Wild-type (LRP5+/+), heterozygous (LRP5+/−), and homozygous (LRP5−/−) mice were born with frequencies predicted by simple Mendelian ratios. In contrast to the severe developmental defects of LRP6 mutant mice (3), LRP5−/− mice of both sexes developed and appeared normal, gaining weight at a rate equal to that of LRP5+/+ mice and were normally fertile. Under light-

microscopic examination of LRP5-deficient males, there were no apparent histological abnormalities in the tissues examined, including bone, brain, eye, kidney, liver, and pancreas.

Although no apparent low-bone-mass phenotype was observed in 3- to 6-month-old LRP5−/− males under light-microscopic examination, we noticed that the femur and parietal bones were thin and fragile in LRP5−/− females older than 6 months. The thickness of the parietal portion of calvaria of LRP5−/− mice was significantly reduced to 50–60% of the controls ($n = 3$, $P < 0.04$; Fig. 6, which is published as supporting information on the PNAS web site). Similarly, the thickness of tibias of LRP5−/− females was also reduced to 60–70% of the controls (data not shown). We also found some cases of pathological fracture of lower limbs in these mice. Recently, Kato *et al.* (13) generated LRP5−/− mice developing a severe low-bone-mass phenotype similar to that of patients with osteoporosis-pseudoglioma syndrome. The low-bone-mass phenotype of LRP5−/− generated by Kato *et al.* was observed regardless of sex and age, and a significant number of the mice died within the first month of life because of fractures. The relatively modest bone phenotype of our LRP5−/− females resembles the osteoporosis of humans and suggests that the involvement of other factors, including sex, aging, hormonal status, dietary exposure, and genetic background in the development of a low-bone-mass phenotype.

Impaired Chylomicron Clearance. To determine the metabolic consequences of LRP5 deficiency, we analyzed the effects of LRP5 deficiency on lipoprotein metabolism by using LRP5−/−, +/−, and +/+ mice. The plasma levels of cholesterol in LRP5+/− and LRP5−/− mice that were fed a standard laboratory chow were identical to those of their LRP5+/+ littermates (Fig. 7, which is published as supporting information on the PNAS web site). In contrast, when mice were fed a high-fat diet containing 7.5% coconut oil and 1.25% cholesterol, plasma cholesterol levels were significantly increased in both LRP5+/− and LRP5−/− mice. The levels of plasma cholesterol in LRP5−/− mice fed a high-fat diet for 2 months were ≈200 mg/dl, whereas those in LRP5+/+ littermates were ≈170 mg/dl (Fig. 2*A*). HPLC analysis of the plasma lipoprotein profile revealed that very low-density lipoprotein cholesterol was increased in LRP5−/− mice after being fed a high-fat diet (Fig. 7). The levels of plasma triglyceride in LRP5+/+ and −/− mice were indistinguishable (within the range of 50–80 mg/dl).

apoE-containing chylomicron remnants can be cleared normally in LDL receptor-lacking familial hypercholesterolemia patients and Watanabe hereditary hyperlipidemic rabbits (29). To determine the effects of LRP5 deficiency on the plasma clearance of chylomicron remnants, we injected fluorescently labeled chylomicron remnants into LRP5−/− mice and +/+ littermates fed a high-fat diet. As shown in Fig. 2*B*, approximately half of the injected chylomicron remnants were cleared from the plasma of LRP5+/+ mice at 30 min after injection, whereas >80% remained in the plasma of LRP5−/− mice. Consistent with the delayed clearance, hepatic uptake of the injected fluorescence was markedly reduced in LRP5−/− mice (≈16% of LRP5+/+ mice, Fig. 2*C*). A similar result was obtained for apoE-rich β-migrating very low-density lipoprotein (data not shown). The mRNA levels of LDL receptor and LRP1 (a candidate chylomicron remnant receptor; ref. 30), were indistinguishable between LRP5+/+ and −/− mice (data not shown). These data indicate that LRP5 recognizes apoE-containing lipoproteins *in vivo* and plays a role in the hepatic clearance of chylomicron remnants.

Impaired Glucose-Induced Insulin Secretion. We next analyzed the effects of LRP5 deficiency on glucose metabolism in LRP5−/− mice. Mice were fed either a normal laboratory chow diet (CE-2, CLEA Japan, Osaka) or a high-fat diet containing 1.5% cholesterol, 7.5% olive oil, 5% cholic acid, and 7.5% milk casein in a standard

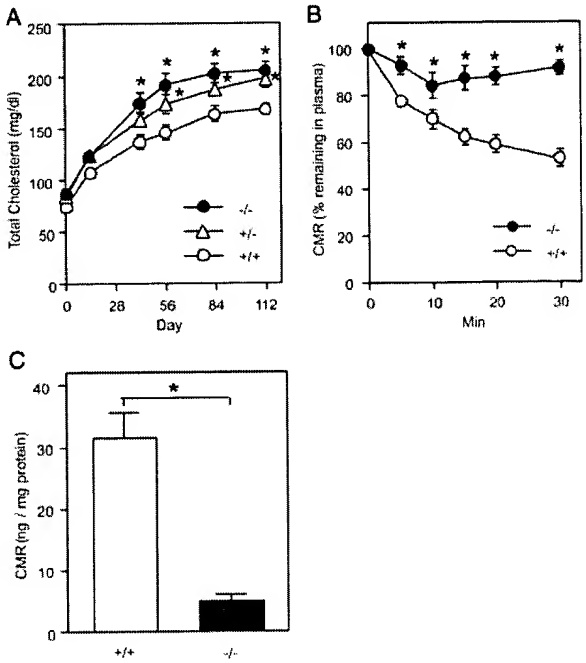

Fig. 2. Diet-induced hypercholesterolemia in LRP5-deficient mice. (*A*) Total plasma cholesterol levels in mice that were fed a high-fat diet. Mice (7–8 weeks of age) heterozygous (LRP5+/−) and homozygous (LRP5−/−) for LRP5 deficiency and their wild-type littermates (LRP5+/+) were fed a high-fat diet for 16 weeks, during which plasma total cholesterol levels of each mouse were measured at the indicated times. The values are the mean ± SE for six mice. *, $P < 0.05$ compared with LRP5+/+. (*B* and *C*) Plasma clearance (*B*) and liver uptake (*C*) of injected chylomicron remnants (CMR). The values are the mean ± SE for six mice. *, $P < 0.01$; Student's *t* test.

laboratory chow diet. Although fasted blood glucose and insulin levels in LRP5−/− and +/− mice appeared identical to those of their +/+ littermates, even after being fed a high-fat diet (90–110 mg/dl), LRP5−/− and LRP5+/− mice exhibited impaired glucose tolerance (IGT) during an i.p. glucose-tolerance test (Fig. 3*A*). This IGT was observed regardless of sex; however, it was age-dependent, because significant glucose intolerance was not seen in LRP5-deficient mice before 6 months of age. Consistent with the marked glucose intolerance, the glucose-induced increase in plasma insulin concentration was lower in both LRP5−/− and LRP5+/− mice than in LRP5+/+ mice (Fig. 3*B*). Pancreatic sections from 6-month-old LRP5+/+ and LRP5−/− mice showed no manifestation of insulitis, including the infiltration of lymphocytes or reduced cell mass in LRP5−/− islets (Fig. 8*A*, which is published as supporting information on the PNAS web site). Similarly, the appearances of alpha and beta cells of the islets were almost indistinguishable in LRP5+/+ and −/− mice as determined by Grimelius (alpha cells; Fig. 8*B*) and aldehyde–fuchsin staining (beta cells; Fig. 8*C*). Pancreatic insulin levels in LRP5−/− mice were not significantly different from those of LRP5+/+ mice and are as follows: 7.07 ± 0.94 and 6.40 ± 0.48 milliunits/mg of protein in LRP5+/+ and LRP5−/− mice, respectively ($n = 6$; Fig. 8*D*). Pancreas weights were also indistinguishable in LRP5+/+ and −/− mice (306 ± 17 and 296 ± 8 mg in LRP5+/+ and LRP5−/− mice, respectively, $n = 6$). No apparent differences were seen in the size of the islets between LRP5+/+ and −/− mice either, as shown in Table 3, which is published as supporting information on the PNAS web site. An i.p. insulin tolerance test revealed that LRP5−/− mice fed a normal diet were not insulin resistant (data not shown). In contrast to LRP5−/− mice, IGT was not seen in mice lacking apoE (data not shown), suggesting that the IGT in

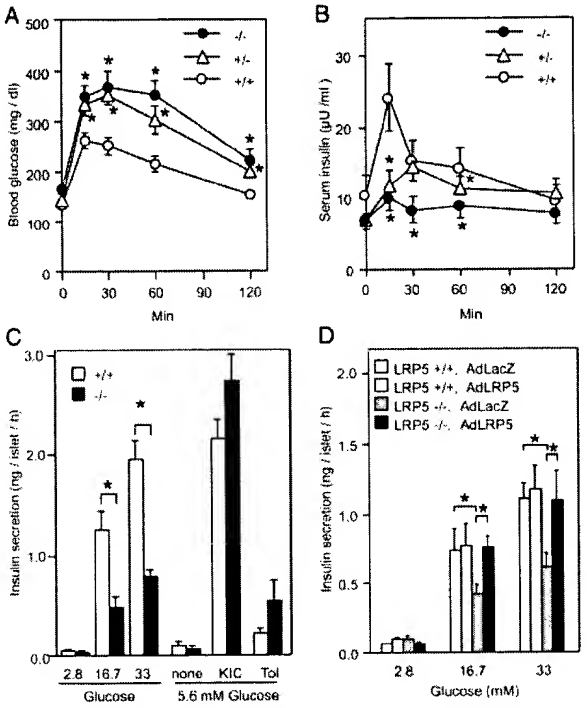

Fig. 3. Impaired glucose-induced insulin secretion in LRP-deficient mice and amelioration by AdLRP5. (*A* and *B*) Blood glucose (*A*) and serum insulin (*B*) levels in LRP5+/+, +/−, and −/− mice after glucose injection. (*C*) Impaired insulin secretion from the islets of LRP5−/− mice. Insulin secretion was induced by different concentrations of glucose and 0.2 mM tolbutamide (Tol), or 10 mM α-ketoisocaproate (KIC), in the presence of 5.6 mM glucose. (*D*) Restoration of insulin secretion by AdLRP5. Pancreatic islets were isolated from LRP5+/+ and −/− mice, infected with recombinant adenoviruses encoding LRP5 (AdLRP5) or LacZ (AdLacZ), and insulin secretion was measured at various glucose concentrations. The values in *A* and *B* are the mean ± SE for six mice; those in *C* and *D* are the mean ± SE for four mice. *, $P < 0.01$; Student's *t* test.

LRP5+/− and −/− mice is independent of apoE binding to LRP5. Although LRP5−/− islets showed impaired glucose-induced insulin secretion, no apparent insulin resistance was observed in LRP5−/− mice. Other factors, including aging, obesity, and prolonged high-fat feeding, may therefore be required to induce typical type 2 diabetes in LRP5−/− mice.

To further define the effects of LRP5 deficiency on glucose-induced insulin secretion, pancreatic islets were prepared from LRP5+/+ and −/− mice, and the changes in the levels of glucose-induced insulin secretion were analyzed. Consistent with the glucose-tolerance test, the change in the insulin secretory response to glucose in LRP5−/− islets was profoundly lower than that of LRP5+/+ islets, particularly at higher concentrations (Fig. 3*C*). When islets were incubated with 10 mM α-ketoisocaproate, which is used for ATP production (31), the changes in the levels of insulin secretion from islets of LRP5−/− mice were approximately the same as those from LRP5+/+ mice, suggesting that there is no impaired ATP production from α-ketoisocaproate in the mitochondrial tricarboxylic acid cycle. Similarly, when cells were incubated with 0.2 mM tolbutamide, there were no changes in the levels of insulin secretion in LRP5−/− and +/+ mice. To restore the impaired insulin secretory response to glucose, LRP5−/− islets were infected with recombinant adenovirus encoding human LRP5 (AdLRP5). As shown in Fig. 3*D*, infection of LRP5−/− islets with AdLRP5 caused their glucose-induced insulin secretion to recover to the levels of LRP5+/+ islets infected with control adenovirus encoding β-galactosidase (AdLacZ) or AdLRP5.

To further evaluate the impaired glucose-induced insulin secretion in LRP5−/− islets, we compared ATP and ADP levels in the islets. As shown in Table 1, the ATP content and ATP/ADP ratio in the presence of 22.2 mM glucose were significantly decreased (by 25–30%) in LRP5−/− islets compared with those in +/+ islets. In contrast, the glycogen content of the islets and hepatic glycogen synthase activity were almost unaltered in LRP5−/− mice (data not shown). Taken together, these data (Fig. 3*C* and Table 1) suggest that the glycolytic pathway was impaired in the LRP5−/− islets.

Consistent with the decreased ATP content and ATP/ADP ratio, glucose-induced intracellular $[Ca^{2+}]_i$ level was markedly decreased in uninfected LRP5-deficient islets. Fig. 4 *A* and *B* shows the glucose-induced $[Ca^{2+}]_i$ increase (as determined by changes in fluorescence intensity) in LRP5+/+ and −/−islets infected with AdLacZ or AdLPR5. The glucose-induced $[Ca^{2+}]_i$ increase in LRP5−/− islets infected with AdLacZ (Fig. 4*B*) was markedly lower than that of LRP5+/+ islets infected with AdLacZ or AdLRP5 (Fig. 4*A*). The average changes in fluorescence intensity (in arbitrary units) by glucose (2.8 mM → 20 mM) in LRP5−/− and LRP5+/+ islets infected with AdLacZ were 29.85 ± 4.04 and 11.10 ± 1.36, respectively ($n = 30$; $P < 0.001$). When LRP5-deficient islets were infected with AdLRP5, the glucose-induced $[Ca^{2+}]_i$ was restored almost completely to normal levels (Fig. 4*B*). There were no statistical differences in the increases in $[Ca^{2+}]_i$ among LRP5+/+ islets infected with AdLacZ or AdLRP5 and LRP5−/−islets infected with AdLRP5. We also examined the glucose-induced production of IP3. The glucose-induced intracellular levels of IP3 were profoundly reduced in LRP5−/− islets (Fig. 4*C*). When LRP5-deficient islets were infected with AdLRP5, the glucose-induced IP3 production was restored almost completely to normal levels (Fig. 4*D*).

Real-Time PCR Analysis. To identify the mechanism underlying the impaired glucose-stimulated insulin secretion, especially the reduced glycolytic pathway, we evaluated steady-state mRNA levels of glucose-sensing proteins and the hepatocyte nuclear factor (HNF) family of transcriptional factors by real-time PCR (see *Supporting Methods*). As shown in Table 2, the mRNA levels of insulin-like growth factor (IGF)-1 receptor, insulin receptor

Table 1. ATP and ADP contents and the ATP/ADP ratio in glucose-stimulated islets

	LRP5+/+		LRP5−/−	
Measurement	2.8 mM glucose	22.2 mM glucose	2.8 mM glucose	22.2 mM glucose
ATP, pmol/islet	4.69 ± 0.08	9.95 ± 0.78	5.20 ± 0.16	7.91 ± 0.74*
ADP, pmol/islet	2.66 ± 0.23	1.89 ± 0.07	1.93 ± 0.15	1.81 ± 0.10
ATP/ADP ratio	2.10 ± 0.23	4.93 ± 0.07	2.31 ± 0.12	3.37 ± 0.20**

Islets of four mice were pooled and incubated at 37°C in the presence of 2.8 or 22.2 mM glucose. After 1 h, the incubation was stopped by the addition of 0.125 ml of trichloroacetic acid to a final concentration of 5%. The islets were disrupted by sonication, and ATP and ADP contents were measured with a luciferase–luciferin system (25). Data are from four independent experiments. Each value represents the mean ± SE. *, $P < 0.01$; **, $P < 0.001$; as compared with wild-type islets (one-way ANOVA).

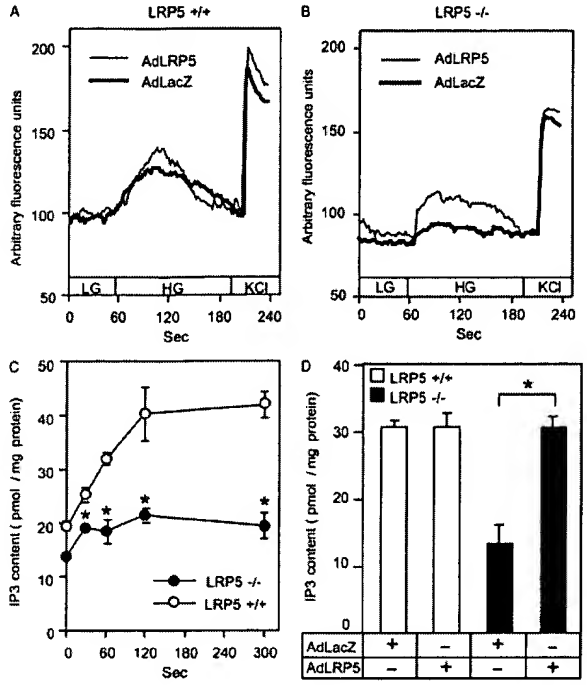

Fig. 4. Impaired glucose-induced $[Ca^{2+}]_i$ increase and IP3 production in LRP5-deficient islets. (*A* and *B*) LRP5+/+ (*A*) and −/− (*B*) islets infected with AdLRP5 or control AdLacZ. Changes in $[Ca^{2+}]_i$ were measured under low glucose (2.8 mM; LG), high glucose (20 mM; HG), or 20 mM KCl (KCl). Representative data from 30 experiments are shown. (*C*) Time course of IP3 content in response to 20 mM glucose in LRP5+/+ and −/− islets. Values are the mean ± SE from quadruplicate determinations. (*D*) Restoration of IP3 production by AdLRP5. Pancreatic islet cells were isolated from LRP5+/+ and −/− mice and infected with AdLRP5 or AdLacZ, and the IP3 content was measured at 5 min after exposure to 20 mM glucose. The values are the mean ± SE from quadruplicate determinations. *, $P < 0.01$; Student's *t* test.

substrate-2 (IRS-2), HNF-4α, insulin receptor, and Tcf1 (HNF-1α) transcripts were drastically decreased in LRP5−/− islets (3%, 6%, 9%, 12%, and 17% of control, respectively). Similarly, the levels of Tcf2 (HNF-1β), glucokinase, Foxa1 (Forkhead box A1, HNF-3α), and Tcf4 transcripts were profoundly decreased in LRP5−/− islets (33%, 49%, 51%, and 59% of control, respectively). In contrast, the levels of glucose transporter 2 were unchanged and the insulin transcripts were increased by 30% in LRP5−/− islets.

Effects of Wnt on Glucose-Induced Insulin Secretion. LRP5 has been shown to bind Wnt and believed to act as a coreceptor for the Wnt signaling pathway. To determine the involvement of Wnt proteins in glucose-induced insulin secretion, we pretreated LRP5+/+ islets with CM from Wnt-3a-, Wnt-5a-, or parental vector-transfected L cells (neo-CM) (27). As shown in Fig. 5*A*, pretreatment of LRP5+/+ islets with Wnt-3a-, and Wnt-5a CM for 16 h markedly stimulated glucose-induced insulin secretion. This Wnt protein-stimulated glucose-induced insulin secretion was blocked by the addition of purified Frizzled-related protein-1 (*FRP1* gene product), a soluble antagonist for sFRP-1 (28).

In contrast, this stimulation of glucose-induced insulin secretion by Wnt-3a-CM was not seen in uninfected LRP5-deficient islets (data not shown) or in LRP5−/− islets infected with AdLacZ, whereas AdLRP5 infection restored the Wnt-3a-stimulated insulin secretion (Fig. 5*B*). These data demonstrate that Wnt-3a-stimulated glucose-induced insulin secretion is mediated by LRP5. In contrast to the stimulation by Wnt-3a of glucose-induced insulin secretion, the intracellular insulin levels

Table 2. Relative amounts of mRNAs in islets from LRP5−/− mice as compared with values in +/+ mice

mRNA from islets	Relative amount of mRNA in LRP5−/− mice
Tcf1 (HNF-1α)	0.17
Tcf2 (HNF-1β)	0.33
Tcf4	0.59
Foxa1 (HNF-3α)	0.51
Foxa2 (HNF-3β)	0.85
HNF-4α	0.09
Insulin	1.30
IRS-1	0.60
IRS-2	0.06
Insulin receptor	0.12
IGF-1	1.78
IGF-2	0.64
IGF-1 receptor	0.03
Glucose transporter 2	0.94
Glucokinase	0.49
LRP5	0.01

Male mice aged 6–8 months were used in this experiment. Total RNA from islets of four mice was pooled and subjected to real-time PCR quantification as described under *Experimental Procedures*. Cyclophilin was used as the invariant control. Values represent the amount of mRNA relative to that in LRP5+/+ mice, which is arbitrarily defined as 1.

were unchanged, indicating that Wnt-3a has no effects on the production of insulin in the islets (data not shown).

Discussion

Here, we investigated the function of LRP5 by examining LRP5−/− mice. We show that LRP5 is required for proper hepatic clearance of chylomicron remnants and for glucose-induced insulin secretion from the pancreatic islets, in addition to bone and eye development. Hyperlipoproteinemia has long been known to be a significant complication of diabetes, and our studies suggest a possible molecular linkage through LRP5. So far, the LRP5 locus has been linked to type 1 diabetes (32, 33) in humans, and our studies indicate that a more detailed investigation of the linkage of LRP5 with type 2 diabetes is warranted.

Consistent with the impaired glucose-induced insulin secretion and the reduced ATP/ADP ratio in LRP5−/− islets, the

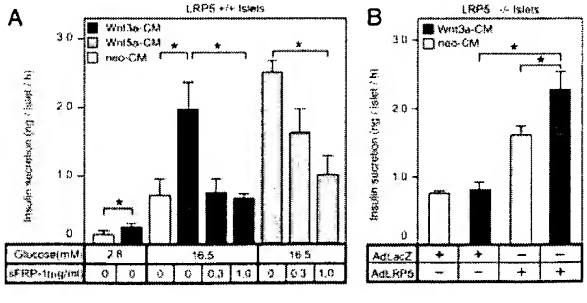

Fig. 5. Effects of Wnt-3a and Wnt-5a on glucose-induced insulin secretion. (*A*) Insulin secretion from the islets. LRP5+/+ islets were pretreated with 5-fold diluted Wnt-3a-CM, Wnt-5a-CM, or control neo-CM in the presence of the indicated concentration of sFRP-1 for 16 h before measuring insulin secretion induced by glucose. (*B*) Lack of Wnt-3a stimulation of insulin secretion from LRP5-deficient islets and restoration by AdLRP5. LRP5−/− islets were infected with AdLRP5 or AdLacZ and exposed to Wnt-3a- or control neo-CM for 16 h before measuring insulin secretion in the presence of 16.5 mM glucose. The values are the mean ± SE for four mice from quadruplicate determinations. *, $P < 0.01$; Student's *t* test.

steady-state levels of mRNAs for several important molecules in the islets were profoundly decreased. These include the HNF family of transcriptional factors (Tcf1, Tcf2, Foxa1, and HNF-4α,), glucose-sensing protein (glucokinase), and insulin-signaling proteins (insulin receptor, IGF-1 receptor, and IRS-2). Mutations in Tcf1, Tcf2, and HNF-4α genes impair insulin secretion and cause mature-onset diabetes of the young (MODY). Insulin signaling through the insulin receptor is important for maintaining the transcriptional level of glucokinase and insulin itself in beta cells (34–36). Also, the IGF-1 receptor signaling pathway through IRS-2 mediates the beta cell compensation for peripheral insulin resistance, as well as the development, proliferation, and survival of beta cells (37, 38). Our data provide the evidence that LRP5 together with Wnt maintains the normal function of the β cells through the transcriptional regulation of the above-mentioned genes.

Glycogen synthase kinase β (GSK3β) is a key component in many biological processes, including insulin- and Wnt-signaling pathways. Both insulin and Wnt inactivate GSK3β although through different mechanisms: phosphorylation mediated by Akt/PKB and axin conduction complex, respectively. Whereas insulin induces glycogen synthase activity through the inactivation of GSK3β, Wnt had no effect on glycogen synthase activity (39). Despite the marked reduction of steady-state insulin receptor transcripts in LRP5$-/-$ islets, the glycogen content of the islets, hepatic glycogen synthase activity, and pancreatic insulin content were almost unchanged in LRP5$-/-$ mice. In the beta cell-specific knockout for the insulin receptor, there is a decrease in glucose-stimulated insulin release and a marked reduction the insulin content of the cells (35). In contrast, the insulin content in the islets is unaltered in the beta cell-specific knockout for IGF receptor, whereas glucose-stimulated insulin secretion is markedly impaired (38). Based on the similarity of glucose-sensing defects between the mice lacking LRP5 and beta cell-specific IGF receptor, and the drastic reduction of IGF receptor transcripts in LRP5$-/-$ islets, it is suggested that IGF signaling is impaired in LRP5$-/-$ islets.

Despite the differences in the biological roles of Wnt-3a and Wnt-5a (β-catenin/Wnt pathway and Ca^{2+}/Wnt pathway, respectively), both proteins have similar effects on the stimulation of glucose-induced insulin secretion. Based on the stimulation of glucose-induced insulin secretion by Wnt proteins and the lack of the Wnt-stimulated insulin secretion in LRP5 deficient islets, we conclude that LRP5 together with Wnt proteins modulates glucose-induced insulin secretion. Although the precise pathway for Wnt signaling in the islets is currently unknown, this work has demonstrated that Wnt proteins are involved in normal glucose metabolism in the adult mouse and suggests that the Wnt pathway may provide novel therapeutic strategies for the treatment of type 2 diabetes.

We thank Drs. M. S. Brown and J. L. Goldstein for helpful discussion and critical reading of this manuscript; T. F. Osborne, P. Espenshade, H. Okamoto, H. Takeshima, and S. Takasawa for helpful advice; I. Gleadall for review of the manuscript; J. Rubin for sFRP-1 plasmid; A. Yamashita and T. Kadowaki for valuable advice on ATP and ADP measurement; S. Iwasaki for excellent technical advice on the glycogen measurement; H. Iguchi for technical help with real-time PCR; K. Katoh for assistance with Ca^{2+} measurement; and Y. Takei, M. Sasaki, S. Takahashi, and R. Nagata for excellent technical assistance. This work was supported in part by Japan Society for Promotion of Science Grant RFTF97L00803 and Japan Science and Technology Corporation/Exploratory Research for Advanced Technology (Yanagisawa Orphan Receptor Project).

1. Wehrli, M., Dougan, S. T., Caldwell, K., O'Keefe, L., Schwartz, S., Vaizel-Ohayon, D., Schejter, E., Tomlinson, A. & DiNardo, S. (2000) *Nature* **407,** 527–530.
2. Tamai, K., Semenov, M., Kato, Y., Spokony, R., Liu, C., Katsuyama, Y., Hess, F., Saint-Jeannet, J. P. & He, X. (2000) *Nature* **407,** 530–535.
3. Pinson, K. I., Brennan, J., Monkley, S., Avery, B. J. & Skarnes, W. C. (2000) *Nature* **407,** 535–538.
4. Bafico, A., Liu, G., Yaniv, A., Gazit, A. & Aaronson, S. A. (2001) *Nat. Cell Biol.* **3,** 683–686.
5. Mao, J., Wang, J., Liu, B., Pan, W., Farr, G. H., III, Flynn, C., Yuan, H., Takada, S., Kimelman, D., Li, L. & Wu, D. (2001) *Mol. Cell* **7,** 801–809.
6. Mao, B., Wu, W., Li, Y., Hoppe, D., Stannek, P., Glinka, A. & Niehrs, C. (2001) *Nature* **411,** 321–325.
7. Nusse, R. & Varmus, H. E. (1992) *Cell* **69,** 1073–1087.
8. Wodarz, A. & Nusse, R. (1998) *Annu. Rev. Cell Dev. Biol.* **14,** 59–88.
9. Sparks, A. B., Morin, P. J., Vogelstein, B. & Kinzler, K. W. (1998) *Cancer Res.* **58,** 1130–1134.
10. Bhanot, P., Brink, M., Samos, C. H., Hsieh, J. C., Wang, Y., Macke, J. P., Andrew, D., Nathans, J. & Nusse, R. (1996) *Nature* **382,** 225–230.
11. Ross, S. E., Hemati, N., Longo, K. A., Bennett, C. N., Lucas, P. C., Erickson, R. L. & MacDougald, O. A. (2000) *Science* **289,** 950–953.
12. Gong, Y., Slee, R. B., Fukai, N., Rawadi, G., Roman-Roman, S., Reginato, A. M., Wang, H., Cundy, T., Glorieux, F. H., Lev, D., *et al.* (2001) *Cell* **107,** 513–523.
13. Kato, M., Patel, M. S., Levasseur, R., Lobov, I., Chang, B. H., Glass, D. A., Jr., Hartmann, C., Li, L., Hwang, T. H., Brayton, C. F., *et al.* (2002) *J. Cell Biol.* **157,** 303–314.
14. Little, R. D., Carulli, J. P., Del Mastro, R. G., Dupuis, J., Osborne, M., Folz, C., Manning, S. P., Swain, P. M., Zhao, S. C., Eustace, B., *et al.* (2002) *Am. J. Hum. Genet.* **70,** 11–19.
15. Boyden, L. M., Mao, J., Belsky, J., Mitzner, L., Farhi, A., Mitnick, M. A., Wu, D., Insogna, K. & Lifton, R. P. (2002) *N. Engl. J. Med.* **346,** 1513–1521.
16. Hey, P. J., Twells, R. C., Phillips, M. S., Yusuke, N., Brown, S. D., Kawaguchi, Y., Cox, R., Guochun, X., Dugan, V., Hammond, H., *et al.* (1998) *Gene* **216,** 103–111.
17. Figueroa, D. J., Hess, J. F., Ky, B., Brown, S. D., Sandig, V., Hermanowski-Vosatka, A., Twells, R. C., Todd, J. A. & Austin, C. P. (2000) *J. Histochem. Cytochem.* **48,** 1357–1368.
18. Kim, D. H., Inagaki, Y., Suzuki, T., Ioka, R. X., Yoshioka, S. Z., Magoori, K., Kang, M. J., Cho, Y., Nakano, A. Z., Liu, Q., *et al.* (1998) *J. Biochem. (Tokyo)* **124,** 1072–1076.
19. Yagi, T., Nada, S., Watanabe, N., Tamemoto, H., Kohmura, N., Ikawa, Y. & Aizawa, S. (1993) *Anal. Biochem.* **214,** 77–86.
20. Yagi, T., Tokunaga, T., Furuta, Y., Nada, S., Yoshida, M., Tsukada, T., Saga, Y., Takeda, N., Ikawa, Y. & Aizawa, S. (1993) *Anal. Biochem.* **214,** 70–76.
21. Abrahamsohn, P. A. & Zorn, T. M. (1993) *J. Exp. Zool.* **266,** 603–628.
22. Redgrave, T. G. & Martin, G. (1977) *Atherosclerosis (Shannon, Irel.)* **28,** 69–80.
23. Takahashi, S., Kawarabayasi, Y., Nakai, T., Sakai, J. & Yamamoto, T. (1992) *Proc. Natl. Acad. Sci. USA* **89,** 9252–9256.
24. Becker, T. C., BeltrandelRio, H., Noel, R. J., Johnson, J. H. & Newgard, C. B. (1994) *J. Biol. Chem.* **269,** 21234–21238.
25. Katoh, K., Komatsu, T., Yonekura, S., Ishiwata, H., Hagino, A. & Obara, Y. (2001) *J. Endocrinol.* **169,** 381–388.
26. Detimary, P., Van den Berghe, G. & Henquin, J. C. (1996) *J. Biol. Chem.* **271,** 20559–20565.
27. Shibamoto, S., Higano, K., Takada, R., Ito, F., Takeichi, M. & Takada, S. (1998) *Genes Cells* **3,** 659–670.
28. Uren, A., Reichsman, F., Anest, V., Taylor, W. G., Muraiso, K., Bottaro, D. P., Cumberledge, S. & Rubin, J. S. (2000) *J. Biol. Chem.* **275,** 4374–4382.
29. Kita, T., Goldstein, J. L., Brown, M. S., Watanabe, Y., Hornick, C. A. & Havel, R. J. (1982) *Proc. Natl. Acad. Sci. USA* **79,** 3623–3627.
30. Rohlmann, A., Gotthardt, M., Hammer, R. E. & Herz, J. (1998) *J. Clin. Invest.* **101,** 689–695.
31. Ashcroft, S. J. (1997) *Adv. Exp. Med. Biol.* **426,** 73–80.
32. Nakagawa, Y., Kawaguchi, Y., Twells, R. C., Muxworthy, C., Hunter, K. M., Wilson, A., Merriman, M. E., Cox, R. D., Merriman, T., Cucca, F., *et al.* (1998) *Am. J. Hum. Genet.* **63,** 547–556.
33. Twells, R. C., Metzker, M. L., Brown, S. D., Cox, R., Garey, C., Hammond, H., Hey, P. J., Levy, E., Nakagawa, Y., Philips, M. S., *et al.* (2001) *Genomics* **72,** 231–242.
34. Leibiger, I. B., Leibiger, B., Moede, T. & Berggren, P. O. (1998) *Mol. Cell* **1,** 933–938.
35. Kulkarni, R. N., Bruning, J. C., Winnay, J. N., Postic, C., Magnuson, M. A. & Kahn, C. R. (1999) *Cell* **96,** 329–339.
36. Leibiger, B., Leibiger, I. B., Moede, T., Kemper, S., Kulkarni, R. N., Kahn, C. R., de Vargas, L. M. & Berggren, P. O. (2001) *Mol. Cell* **7,** 559–570.
37. Withers, D. J., Burks, D. J., Towery, H. H., Altamuro, S. L., Flint, C. L. & White, M. F. (1999) *Nat. Genet.* **23,** 32–40.
38. Kulkarni, R. N., Holzenberger, M., Shih, D. Q., Ozcan, U., Stoffel, M., Magnuson, M. A. & Kahn, C. R. (2002) *Nat. Genet.* **31,** 111–115.
39. Ding, V. W., Chen, R. H. & McCormick, F. (2000) *J. Biol. Chem.* **275,** 32475–32481.